Influence of grain size on distribution of temperature and thermal stress in ZnO varistor ceramics

CHEN Qingheng (陈青恒)[1], HE Jinliang (何金良)[1], TAN Kexiong (谈克雄)[1], CHEN Shuiming (陈水明)[1], YAN Minyu (严民昱)[2] & TANG Jianxin (唐建新)[3]

1. Department of Electrical Engineering, Tsinghua University, Beijing 100084, China;
2. Department of Material Science, Tsinghua University, Beijing 100084, China;
3. Beijing Institute of Aerial Materials, Beijing 100084, China
Correspondence should be addressed to Chen Qingheng(email: chengh00@mails.tsinghua.edu.cn)

Received February 26, 2002

Abstract The nonuniformity of temperature distribution within ZnO varistor ceramics would decrease its energy absorption capability. In this paper, the distributions of current, temperature and thermal stress within the microstructures of ZnO varistor ceramics are simulated using Voronoi diagram models. The results show that the current concentrates through a few paths in ZnO varistor due to the nonuniformity of ZnO grain size and the variety of electrical characteristics of grain boundaries, which induces local high temperature and great thermal stress when injecting impulse current into ZnO varistor, and leads to melting puncture or cracking failure. The influence of the ZnO grain size on the distributions of temperature and thermal stress within ZnO varistor ceramics is analyzed in detail. The energy absorption capability of ZnO varistor ceramics can be greatly improved by increasing the uniformity of ZnO grain size or decreasing the average size of ZnO grains.

Keywords: ZnO varistor ceramics, Voronoi diagram, current, temperature, thermal stress.

ZnO varistor ceramics is a kind of polycrystalline ceramics, fabricated by sintering ZnO powder with small amount of other metal oxide additives such as Bi_2O_3, Co_2O_3, MnO and Sb_2O_3. With highly nonlinear current-voltage (*I-V*) characteristics, ZnO varistors are widely used as functional elements of arresters for circuit protection against surges. The primary function of ZnO varistors is to clamp the transient voltage to a level that is not harmful to the protected electrical or electronic devices and systems, and at the same time, the ZnO varistors absorb the transient surge energy. When ZnO varistors absorb superfluous surge energy, they may be damaged in three different models: thermal runaway, puncture and cracking. Thermal runaway is due to the negative temperature coefficient of their *I-V* characteristic when they operate in the low electrical field region. If the thermal balance of a ZnO varistor is broken after it absorbs enough surge energy, its temperature rise runs into a vicious cycle, causing unrecoverable damage. Puncture and cracking are referred to as impulse failure in this paper. In puncture failure, a small hole results from melting of the ZnO varistor body where high current concentrates. When a larger current flows through the ZnO varistor, the temperature of some region within the ceramics will rise to or higher than 820℃ at which the Bi_2O_3 in the grain boundary becomes melted and the barriers in the grain

boundary vanish. Then the varistor has a permanent breakdown. At the same time, this highly concentrated current can also generate great temperature gradient, which brings great thermal stress in the ZnO varistors. Cracking failure occurs when the thermal stress is higher than the critical mechanical stress of ZnO varistor ceramics. The local high temperature and thermal stress caused by the nonuniform distribution of current within ZnO varistor ceramics decrease its capability of absorbing surge energy.

Eda[1] and Bartkowiak[2] studied the damage of ZnO varistor ceramics in macrostructures. This paper is to study the effects of the average size of ZnO grains and their uniformity on the distributions of current, temperature, and thermal stress in the microstructures of ZnO varistors. The methods for improving the surge energy absorption capability of ZnO varistor ceramics are discussed, too.

1 Method of simulation

1.1 Model for microstructure of ZnO varistor ceramics

The basic phase is ZnO grain in the microstructure of ZnO varistor ceramics (fig. 1), the grain boundaries between ZnO grains are the origin of the nonlinear *I*-*V* characteristic of ZnO varistor. The grain size varies in the range from 5 to 30 μm, according to its recipe and fabrication technologies. The thickness of grain boundary is about several tens nm.

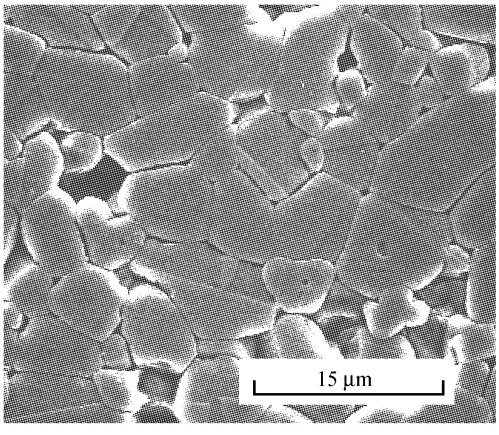

Fig. 1. The microstructure of ZnO varistor ceramics.

Voronoi diagram or Voronoi tessellation is one of the simplest and effective ways to model such a microstructure[3, 4]. The cellular structure underlying the varistor network used in this study is constructed in the following way. Starting with an arbitrary distribution of seed points in a two-dimensional region, we control the number of seeds to meet the demand that the average distance between two adjacent seeds is *s*. The Voronoi vertexes of these seeds are formed by the feature of two-dimension Voronoi network: in a two-dimensional Voronoi network, for every Voronoi vertex q_i, there is, and only is one circumference whose center is q_i and which passes through three or more than three seeds, and at the same time, this circumference is the maximum empty circle without any seed in it. Linking these vertexes we obtain the entire polygon of this seed. When the disorder parameter d=0, the polygons are regular hexagonal cells, which corresponds to the ideal two-dimensional microstructure of ZnO grain. For d>0, the coordinates of seeds deviate from those of d=0. The radius and the angle of the displacement vector were assigned randomly within the intervals [0, $d \times s$] and [0, 2π], respectively.

Figs.1 and 2 show that when disorder parameter $d \geqslant 5$, the 2D Voronoi network is very similar to the planar microstructure of ZnO varistor ceramics. In the simulation, it is assumed that each polygon cell represents a ZnO grain and each edge l_{ij} shared by neighboring cells i and j corresponds to the grain boundary between these two grains. And the thickness of the ceramics is selected as s. The average size of ZnO grain is controlled by s, and the uniformity of ZnO microstructure is determined by disorder parameter d.

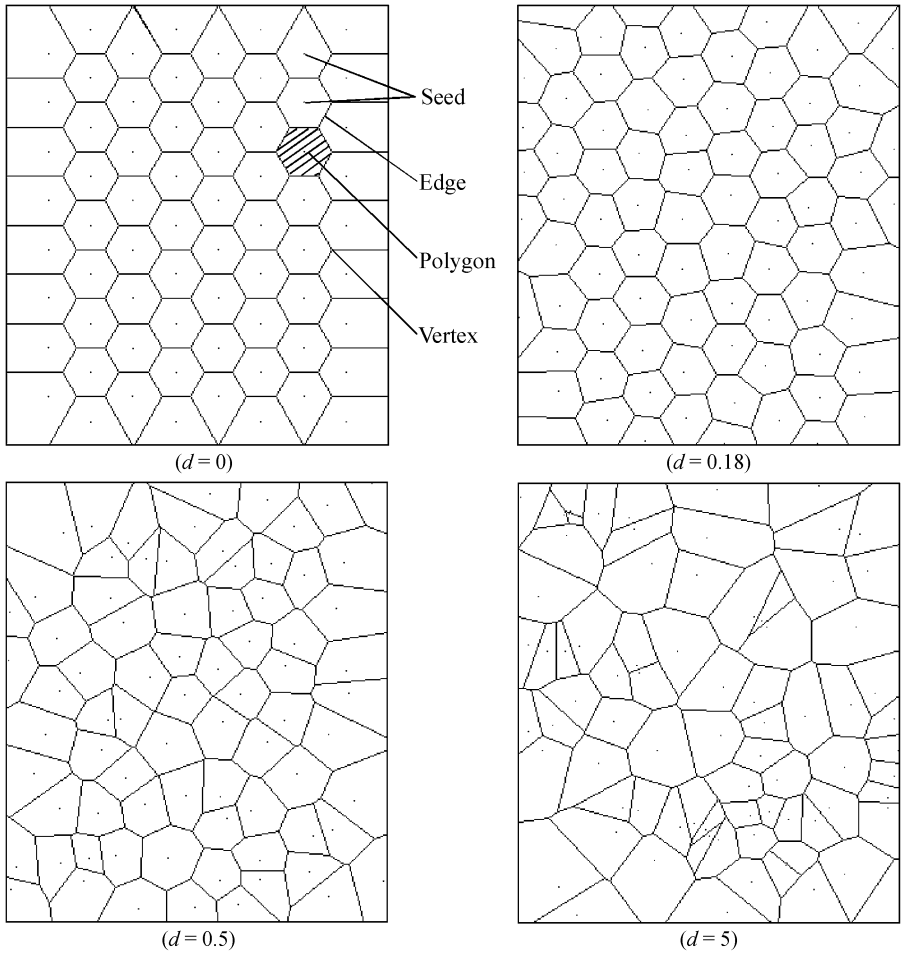

Fig. 2. Voronoi cell structure for different values of disorder parameter d.

1.2 Current and Joule heat in ZnO varistor ceramics

Before calculating the heat generated in ZnO varistor ceramics, the distribution of voltage and current within their microstructures are calculated according to the topology of Voronoi network. A nonlinear resistor network corresponding to the dual of the network of Voronoi polygons is shown in fig.3.

The nonlinear resistor R_{ij} by the real lines as shown in fig.3 is used to describe the electrical characteristic of the grain boundary between grains i and j. The current flowing through the resis-

tor R_{ij} is assumed to be the product of the area ($=l_{ij}\times s$) of the grain boundary and the current density J_{ij} flowing through the grain boundary between grains i and j. According to the conduction mechanism based on the theory of double Schottky barriers, the J-V characteristics of a single grain boundary are modeled by

$$J_{ij}(U_{ij})=\begin{cases}\dfrac{A_1}{\rho_{gh}}\exp\left(-\dfrac{E_g-\beta|U_{ij}|^{\frac{1}{2}}}{K_bT}\right)+A_2\left(\dfrac{|U_{ij}|}{V_B}\right)^a; & |U_{ij}|\leqslant V_{\mathrm{U}},\\ \dfrac{A_1}{\rho_{gb}}\exp\left(-\dfrac{E_g-\beta V_U^{\frac{1}{2}}}{K_bT}\right)+A_2\left(\dfrac{V_U}{V_B}\right)^a+\dfrac{1}{d_{ij}\rho_g}(|U_{ij}|-V_U), & |U_{ij}|>V_{\mathrm{U}}.\end{cases} \tag{1}$$

The first row of (1) corresponds to the I-V characteristics of ZnO varistor in pre-breakdown and breakdown regions within which the current behavior is determined by the thermal activated emission of electrons and the tunneling current; the second row of (1) corresponds to the characteristics in upturn region where the current behavior is determined by the grain resistivity; J_{ij} is the current density as described before, A·cm^{-2}; $U_{ij}=(U_i - U_j)$, U_i and U_j are the voltages of grains i and j, V; d_{ij} is the distance between the centers of the grains i and j, cm. The I-V characteristic of grain boundaries varies very much. From the test results of the barrier voltage and nonlinear coefficient in ref. [5], we found that the barrier voltage V_{B} follows the normal distribution

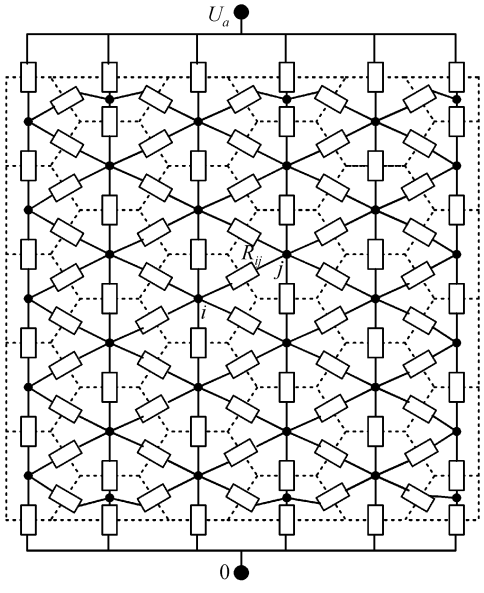

Fig. 3. Circuit for the microscopic simulation of ZnO varistor.

$$p(V_{\mathrm{B}})=\frac{1}{\sqrt{2\pi}\times 0.2}\exp\left[\frac{(V_{\mathrm{B}}-3.2)^2}{2\times 0.2^2}\right],\quad V_{\mathrm{B}}>0;$$

the nonlinear coefficient α follows the distribution $p(\alpha)=\dfrac{1}{\sqrt{2\pi}\times 50}\exp\left[-\dfrac{(\alpha-7)^2}{2\times 50^2}\right]$, $\alpha\geqslant 1$; V_{U} is the critical upturn voltage in high electrical field region, $V_{\mathrm{U}}=V_{\mathrm{B}}(J_{\mathrm{U}}/A_2)^{1/\alpha}$, J_{U} is the critical upturn current in high electrical field region, 10^3A • cm^{-2} is selected in this paper. Other parameters in (1) are shown in table 1.

The voltage is applied between the top and bottom edges of the Voronoi network. The nodal voltage equations are derived from the circuit as shown in fig.3 by the first law of Kirchhoff:

Table 1 The parameters in (1)

Symbol	Meaning	Unit	Value	Symbol	Meaning	Unit	Value
A_1	constant	A • Ω • cm^{-1}	2.5×10^{16}	E_g	barrier height	eV	0.8
A_2	constant	A • Ω • cm^{-2}	0.01	β	constant	eV$^{1/2}$	2.83×10^{-2}
ρ_{gb}	resistivity of grain boundary	Ω • cm	10^{12}	k_B	Boltzmann's constant	J • K^{-1}	1.38×10^{-23}
ρ_g	resistivity of grain	Ω • cm	1	T	temperature	K	300

$$I_i(U)=\sum_{\substack{j=1\\ j\neq i}}^{N+2} l_{ij}s(\mathrm{sign}(U_i-U_j)J_{ij}(U_i-U_j))=0 \quad (i=1 \text{ to } N), \tag{2}$$

where U is the node voltage vector (U_1, U_2, ⋯, U_N); l_{ij} is the length of the common side between grains i and j. If the grain j is not a neighbor of the grain i, then l_{ij}=0. Eq. (2) is a large scale equation set with high nonlinear coefficient. The voltages (U_1, U_2, ⋯, U_N) in (2) are solved by the descending Newton iterative method combined with gradient method. Then the currents passing through grain boundaries can be calculated by (1). The Joule heat consumed at grain boundary is $P_{ij}=sl_{ij}U_{ij}J_{ij}$.

1.3 Method for calculating heat transfer and thermal stress in ZnO varistor ceramics

Every polygon of the Voronoi network is divided into several triangles (fig. 4), and every triangle is uniquely determined by a polygon edge and the center of the polygon. So each triangle is surrounded by three triangles.

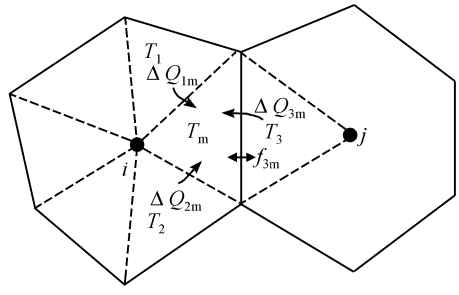

Fig. 4. The schematic diagram of heat transfer.

It is assumed that the average temperature of the triangle m is T_m and its original value is the environmental temperature (300 K in this paper), and the heat (dQ_m) transferring into triangle m during time duration dt is approximately determined by

$$dQ_m=\sum_k dQ_{km}=\sum_k (T_k-T_m)\frac{l_{mk}S}{d_{mk}}k_T dt, \tag{3}$$

where T_k is the average temperature of the adjacent triangle, K; l_{mk} is the length of the common side of two adjacent triangle, cm; d_{mk} is the distance between the centers of the two adjacent triangles, cm; k_T is the thermal conductivity of ZnO varistor ceramics, k_T = 5.7×10^{-2}W • cm^{-1} • K^{-1}[6].

There is one side out of the three sides of each triangle belonging to the edges of the Voronoi polygon. That is to say, it is a grain boundary. So there is a Joule heat power consumption P_m on this edge when a current flows through it. P_m is selected as one half of the Joule heat power of the grain boundary. So the temperature rise dT_m of triangle m during dt is

$$dT_m = \frac{P_m dt + dQ_m}{S_m s \rho C_p}, \tag{4}$$

where S_m is the area of the triangle m, cm^2; s is the thickness of ZnO varistor film, cm; ρ is the mass density of ZnO varistor ceramics, 5.6 g • cm^{-3}; C_p is the thermal capacity of ZnO varistor ceramics, $C_p = 0.498[1+0.000828(T_m-20)]$ J • g^{-1} • K^{-1}[6], $P_m=0.5P_{ij}$.

A set of different equations can be established according to this heat transfer model, and the temperature T_m of triangle m is calculated by finite difference method. If the temperatures of two adjacent triangles are T_m and T_k respectively, then a thermal stress f_{mk} would be formed between them

$$f_{mk} = \frac{Ea(T_m - T_k)}{1-\mu}, \tag{5}$$

where E is the Young's modules of elasticity, α is the linear expansion coefficient of ZnO varistor ceramics, and μ is Poisson's ratio. Since the values of the parameters for ZnO varistors are not available in literature, the corresponding values for porcelain are chosen for the reason that ZnO varistors belong to porcelain. The selected parameters are $\alpha = 4.86\times10^{-6}\,K^{-1}$, μ=0.30, and E= 6.9 $\times10^4$ MPa[7].

2 Result and discussion

2.1 Distributions of current, temperature and thermal stress in ZnO varistor ceramics

The nonuniform growth of ZnO grain during sintering process leads to a variety of ZnO grain sizes and the nonuniformity of microstructure, due to such factors of the fabrication technology of ZnO varistor ceramics as the variety of particle size of raw materials, the unevenly mixed raw materials, the difference in density in the biscuit, and so on. In addition, the additives not evenly mixed also cause the difference in the components, the status and the quantity of current carrier in grain boundaries, which leads to the nonunformity of the *I-V* characteristics of grain boundaries. Because of the high nonlinear coefficient of the *I-V* characteristics of the grain boundaries, the nonuniformity of grain size, and the variety of *I-V* characteristics of grain boundaries, the current flowing through ZnO varistor ceramics is concentrated on some paths with less ZnO grains and higher nonlinear coefficient (so showing lower resistance). Fig. 5(a) shows the current distribution within the model when injecting a 2ms square wave impulse current into ZnO varistor. In fig. 5(a) the gray scale within each polygon represents the relative value of current flowing through it. If there is no or almost no current, the cell is shown as white, while the maximum current is shown as black.

Mizukoshi et al.[8] tested the current distribution on the head surface with a resolution about 1.5 mm. Their result showed that the ratio of the maximum current density to the minimum density is about 2.0. The simulation result of this paper shows that the current distribution is far more nonunform in the microstructure than in macrostructure, and the current is concentrated on the

paths with less ZnO grains(less grain boundaries). For the most serious case, the current is almost concentrated in one path in the model (fig. 5(a)). The grain number in this path is only 70% of the average grain number of other paths in the model. In fig. 5(a), the voltage gradient E is 2.1 kV/cm, and the current passing through the path with black color is 91.2% of the total current.

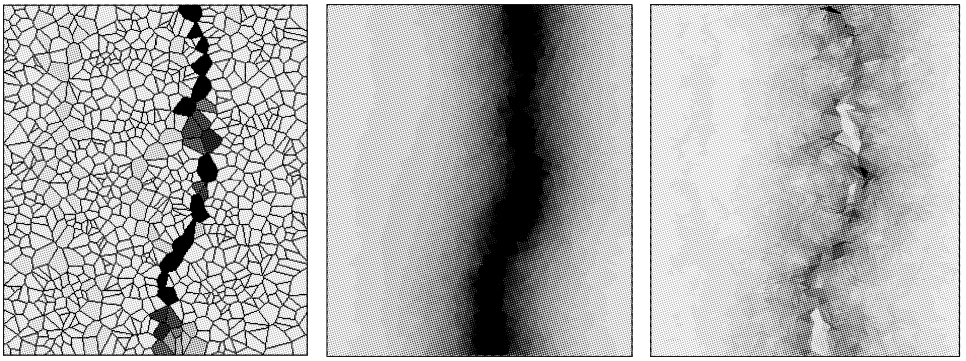

(a) (b) (c)

Fig. 5. Distribution of current (a), temperature (b) and thermal stress (c) within the model when injecting a 2 ms square wave impulse current.

Fig. 5(b) and (c) shows the distributions of temperature and thermal stress when the model carries the current of fig. 5(a) for 2ms. The gray degree represents the relative value of temperature or thermal stress to their maximum, white represents zero and black represents the maximum. From fig. 5(b) we can observe that temperature distribution in ZnO varistor is also nonuniform when injecting an impulse current, and the temperature rises of the regions at or near the ZnO ceramics body where more current is concentrated are far higher than the other parts. It can also be known from fig. 5(c) that the temperature differences among these regions are higher and induce higher thermal stress.

2.2 Influence of uniformity of ZnO grain size on distribution of temperature and thermal stress

In this paper, TR_{av} and TR_{max} are defined as the average and maximum temperature rises on the model, and P_{max} the maximum thermal stress.

The ultimate reason for the nonuniformity of temperature and thermal stress in ZnO varistor ceramic is that the current distribution is not even within its microstructure. Fig. 6 shows the maximum temperature rise and the maximum thermal stress on the simulated model with different disorder parameter d (the average size of cell s = 15 μm). The average current density flowing through the model is about 40 A • cm^{-2}. The uniformity of current distribution decreases with the increasing microstructure nonuniformity of ZnO varistor ceramics, so do the uniformity of temperature rise and thermal stress. For the convenience of comparison, the maximum temperature rise TR_{max} and the maximum thermal stress P_{max} are divided by the average electrical power per unit volume of the current passing through the model.

If the current is absolutely uniform and therefore the heat source is even, there should be no temperature difference and no thermal stress within the microstructure of ZnO varistor. It can be

deduced that the temperature rise should be uniform and increase linearly with time at a speed of 0.36 K • kW^{-1} • cm^3 • ms^{-1}. When $d = 0$, the concentration degree of current is relative uniform in the microstructure of ZnO varistor ceramics, so the maximum temperature rise TR_{max} in the model also increases linearly with the time duration at a speed of about 0.375 K • kW^{-1} • cm^3 • ms which is very close to the case with an absolute uniform distribution of current. Fig. 6 demonstrates that the maximum temperature rise TR_{max} and the maximum thermal stress P_{max} increase with the nonuniform degree of microstructure. 2 ms later, the maximum temperature rise TR_{max} grows from 0.75 to about 2.5 K • kW^{-1} • cm^3 (increasing about 3 times) when d increase from 0 to 5, and the maximum thermal stress P_{max} increases from 0.02 to about 0.3 MPa • kW^{-1} • cm^3 (increasing about 15 times). With the increase of time, P_{max} tends to reach a saturation value, and the increasing speed of TR_{max} reaches 0.36 K • kW^{-1} • cm^3 • ms^{-1}, which shows that the temperature difference within the ceramics reaches a steady status. The more concentrated the current, the longer the time for the temperature difference to reach a steady status.

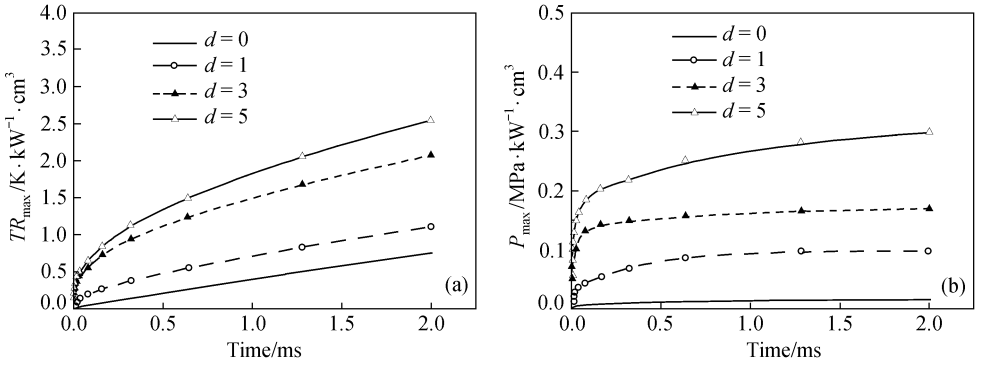

Fig. 6. Relationship between the maximum temperature rise TR_{max}(a), the maximum thermal stress P_{max} (b) and the time on the model with different disorder parameter d.

2.3 Influence of ZnO grain size on distributions of temperature and thermal stress

Besides current distribution, the distributions of temperature and thermal stress within the microstructures of ZnO varistor ceramics are affected by the condition of heat transfer which is determined by the following two factors: the thermal conductivity, and the cooling area and distance within the ceramic. The thermal conductivity of a fixed material is a constant, such as about 5.7×10^{-2} W • cm • K for ZnO varistor ceramics. The cooling area and distance are related to the ZnO grain size beside the current distribution. The cooling area increases and the distance reduces with the decrease in average grain size, thus reducing the time constant for the heat transferr and accelerating heat transfer in ZnO ceramics. The influence of ZnO grain size on the distributions of maximum temperature rise TR_{max} and thermal stress P_{max} on the model with the disorder parameter d=5 are shown in fig.7.

In fig. 7, TR_{max} and P_{max} increase with time duration as in fig. 6. At the time of 2 ms, TR_{max} reaches 1 K • kW^{-1} • cm^3 when the average grain size s = 6 μm, and P_{max} reaches 0.05

MPa •kW^{-1} •cm^3. When s is more than 6 μm, TR_{max} increases at a speed of 0.16 K •kW^{-1} •cm^3 per micrometer, and P_{max} increases at a speed of 0.035 MPa • kW^{-1} • cm^3 per micrometer.

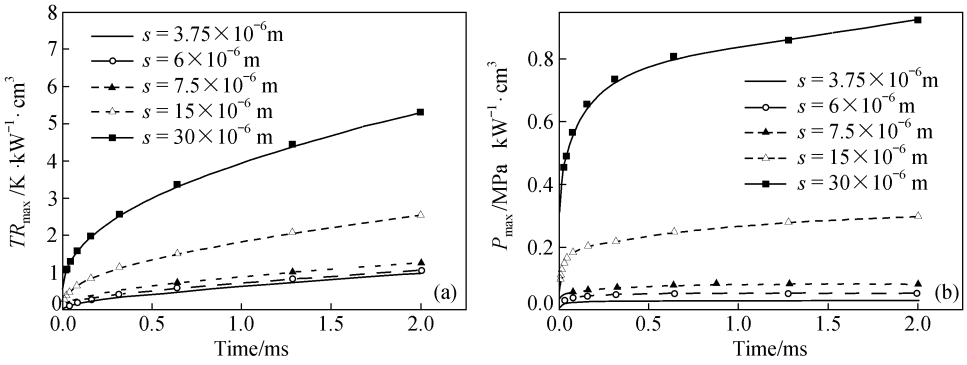

Fig. 7. Variation of the maximum temperature rise TR_{max} and the maximum thermal stress P_{max} with time in the case with different grain sizes (disorder parameter d = 5).

Fig. 7 shows that the temperature difference and thermal stress are greatly decreased when the average size of ZnO grain reduces, thus improving the surge energy adsorption capability of ZnO varistor ceramics. The previous works focused on the improvement of the uniformity of microstructure in order to increase the surge energy adsorption capability. But due to the limitation of the fabrication technology, it is very difficult to achieve good result, while decreasing the average size of ZnO grain is more feasible and effective. Fig.8 shows the microstructures of common and high voltage gradient ZnO varistor under an electron microscope.

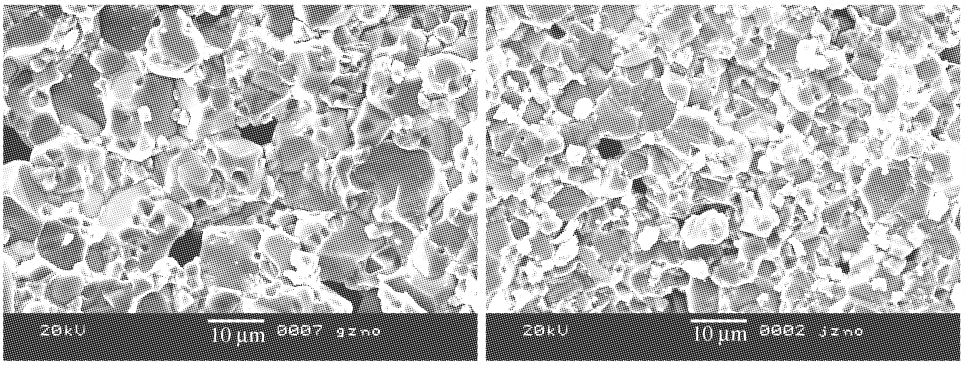

Fig. 8. The microstructure of common and high voltage gradient ZnO varistor under electron microscope.

The average size of ZnO grain of common ZnO varistor ceramics is about 15 μm, while that of high voltage gradient is about 9 μm. The latter is only 0.6 time of the former. The number of ZnO grains and grain boundaries per unit thickness increases when the average grain size reduces, and the voltage-sensitive gradient increases correspondingly. When injecting a current with the same density of the common ZnO varistor into the high voltage gradient one, the surge energy absorbed by it increases proportionally. However, in fact, the permitted current flowing through the high voltage gradient ZnO varistor is far larger than that of a common one. Table 2 shows the

1 mA reference voltage (U_{1mA}) and the surge energy absorption capability of the common and high voltage gradient ZnO varistor used in 10 kV power distribution system. Compared with common type, the 1 mA reference voltage (U_{1mA}) of high voltage gradient ZnO varistor increases 0.4 time, the tolerant value under square wave impulse current increases 0.67 time, and the surge energy absorption capability increases 1.3 times. From fig. 8 we can observe that the uniformity difference in microstructure between these two kinds of ceramics is not significant. The main reason for the improvement on the surge energy absorption capability of the high voltage gradient ZnO varistor is that the number of current paths increases proportionally to the inverse of the square of the average size of ZnO grain, the cooling area increases and the distance decreases correspondingly. All this helps the heat generated in the ceramics to transfer quickly and decrease the temperature difference and thermal stress.

Table 2 Test results of common and high voltage gradient ZnO varistors

ZnO varistor type	Size $D \times h$/mm	U_{1mA}/ kV	2 ms square wave impulse current (18 times) I_{2ms}/A	Surge energy absorption capability (18 times)/J • cm^{-3}
Common	32×30	6.3	120	85
High voltage gradient	32×30	8.8	200	197

3 Conclusion

The distributions of current, temperature and thermal stress in ZnO varistor ceramics were analyzed on Voronoi network model. The results indicate that when an impulse current is injected into ZnO varistor ceramics, local high temperature and thermal stress are induced by the concentrated current caused by the nonuniformity of the microstructure and the varieties of the electrical characteristics of the grain boundaries, which limits the full exploration of surge energy absorption capability.

The results also indicate that we can greatly decrease the temperature difference and the thermal stress in ZnO varistor ceramics by increasing the uniformity of ZnO grain size, or decreasing the average size of ZnO grains, to improve the surge energy absorption capability of the ZnO varistors. The uniformity of ZnO grain size is hard to be improved due to the limitation of the fabrication technology, while the average size of ZnO grain can be controlled by inhibiting the grain growth, which can be realized by adding some other additives, milling the raw material to smaller particles, or decreasing the sintering temperature and so on. The result can provide some constructive instruction on the research of new kinds of ZnO varistor ceramics with higher voltage gradient and larger surge energy absorption capability.

Acknowledgements This work was supported by the National Natural Science Foundation of China (Grant No. 59907001).

References

1. Eda, K., Destruction mechanism of ZnO varistors due to high current, Journal of Applied Physics, 1984, 56(10): 2948—2955.
2. Bartkowiak, M., Comber, M. G., Mahan, G. D., Failure models and energy absorption capability of ZnO varistors, IEEE

Trans. on PWRD, 1999,14: 152—162.

3. Weaire, D., Rivier, N., Soap, cells and statistics-random patterns in two dimensions, Contemp.Phys., 1984, 25(1): 59—99.
4. Bartkowiak, M., Mahan, G. D., Nonlinear currents in Voronoi network, Phys. Rev., 1995, 51(16): 10825—32.
5. Tao, M. , Bui Ai, Dorlanne, O. et al., Different single grain junctions within a ZnO varaistor, J. App. Phys., 1987, 61(4): 1562—1567.
6. Wu, W. H., He, J. L., Gao, Y. M., Properties and Applications of Nonlinear Metal Oxide Varistors (in Chinese), Beijing: Tsinghua University Press, 1998, 166.
7. Koch, R. E., Songster, H. J., Development of a nonfragmenting distribution surge arrester, IEEE Trans. on PAS, 1984, 103(11): 3342—3352.
8. Mizukoshi, A., Cozawa, J., Shirakawa, S. et al., Influence of uniformity on energy absorption capabilities of ZnO oxide elements as applied in arresters, IEEE Trans. on PAS, 1983, 102(5): 1384—1390.